Momentum-resolved electron dynamics of image-potential states on Cu and Ag surfaces

K. Schubert,[1] A. Damm,[1] S. V. Eremeev,[2,3,4] M. Marks,[1] M. Shibuta,[1,5] W. Berthold,[1] J. Güdde,[1] A. G. Borisov,[6,7] S. S. Tsirkin,[3,4] E. V. Chulkov,[4,8] and U. Höfer[1,4]

[1]*Fachbereich Physik und Zentrum für Materialwissenschaften, Philipps-Universität, D-35032 Marburg, Germany*

[2]*Institute of Strength Physics and Materials Science, 634021, Tomsk, Russia*

[3]*Tomsk State University, 634050, Tomsk, Russia*

[4]*Donostia International Physics Center (DIPC), 20018 San Sebastián/Donostia, Basque Country, Spain*

[5]*ERATO, Japan Science and Technology Agency (JST), 3-2-1, Sakado, Takatsu-ku, Kawasaki 213-0012, Japan*

[6]*CNRS, Institut des Sciences Moléculaires d'Orsay, ISMO, Unité de Recherches CNRS-Université Paris-Sud UMR 8214, Bâtiment 351, Université Paris-Sud, F-91405 Orsay Cedex, France*

[7]*Université Paris-Sud, Institut des Sciences Moléculaires d'Orsay, ISMO, Unité de Recherches CNRS-Université Paris-Sud UMR 8214, Bâtiment 351, Université Paris-Sud, F-91405 Orsay Cedex, France*

[8]*Departamento de Física de Materiales UPV/EHU, Centro de Física de Materiales CFM - MPC and Centro Mixto CSIC-UPV/EHU, 20080 San Sebastián/Donostia, Basque Country, Spain*

(Received 15 February 2012; published 15 May 2012)

The dependence of the inelastic lifetime of electrons in the first $n = 1$ image-potential state of clean and rare-gas covered Ag(111), Cu(111), and Cu(100) surfaces on their momentum parallel to the surface has been studied experimentally by means of time- and angle-resolved two-photon photoemission spectroscopy (2PPE) and theoretically by calculations based on the many-body theory within the self-energy formalism. Similar to the previously studied clean Cu(100) surface, the theoretical results are in excellent agreement with the experiment findings for Cu(111). For Ag(111), the theory overestimates the decay rate and its momentum dependence, which is attributed to the neglect of surface plasmon excitations. With increasing parallel momentum, the $n = 1$ state shifts out of the projected bulk band gap on both surfaces and turns into an image-potential resonance. This opens an additional decay channel by resonant electron transfer into the bulk, which is theoretically treated by the application of the wave packet propagation approach. The expected stronger increase of the decay rate upon crossing the edge of the band gap, however, is not observed in the experiment. The decoupling of the image-potential states from the metal surface upon adsorption of rare-gas layers results in a decrease of the decay rate as well as of its momentum dependence by a similar factor, which can be successfully explained by the change of interband and intraband contributions to the total decay rate.

DOI: 10.1103/PhysRevB.85.205431 PACS number(s): 73.20.−r, 79.60.Bm, 78.47.J−

I. INTRODUCTION

Lifetimes of electronic excitations are crucial for many surface phenomena such as electronically induced surface adsorbate reactions or electron transfer across interfaces.[1,2] At metal surfaces, image-potential states have been widely used as a model system to study electron dynamics.[3] The electrons that are excited into these normally unoccupied states are trapped in front of the surface owing to the self-interaction with the polarization charge. Far from the surface, this interaction converges to the classical image potential. When electron penetration into the metal is prohibited by the projected band gap, electron motion in the direction normal to the surface is quantized and the image-potential states form a Rydberg-like series converging toward the vacuum level with energies given by $E_n = -0.85\text{eV}/(n + a)^2$, where $n = 1,2,\ldots$ is the principal quantum number and a the quantum defect. The electron motion parallel to the surface is quasifree with an effective mass m^* close to the free electron mass m_0.

The hydrogen-like character and well defined properties make image-potential states very attractive not only for fundamental experiments but also for theoretical studies of the dynamics of excited states at surfaces. Within the one-electron picture, image-potential states are stationary on the clean metal surfaces. Their population decays because of the interactions with the bath of phonons and metal electrons. Accurate many-body calculations of inelastic electron-phonon and electron-electron scattering processes are available nowadays that have led to a good understanding and quantitative description of the image-potential states' lifetimes.[3] The theory shows that the inelastic scattering processes will, in general, depend on the parallel momentum $k_\parallel$ of the excited electrons. For a comprehensive picture about the different, simultaneously occurring scattering processes it is therefore essential to investigate the decay of the image-potential states as a function of their parallel momentum.

Detailed experimental and theoretical investigations of the momentum-dependent decay of electrons in image-potential states have been done for the clean Cu(100) surface where the inelastic lifetime τ of optically excited electrons has been measured by time- and angle-resolved two-photon photoemission (2PPE) and calculated by evaluating the electron self-energy within the GW approximation.[4] It was shown that the momentum dependence of the inelastic electron-electron decay rate $\Gamma^{e\text{-}e} = 1/\tau$ is governed by interband and intraband decay processes. The momentum dependence of the interband decay results from the energy and momentum dependence of the electron-electron interaction as well as from a $k_\parallel$ dependence of the image-potential state wave functions due to the dispersion of the bulk bands. The intraband decay within the bands of the image-potential states for large $k_\parallel$

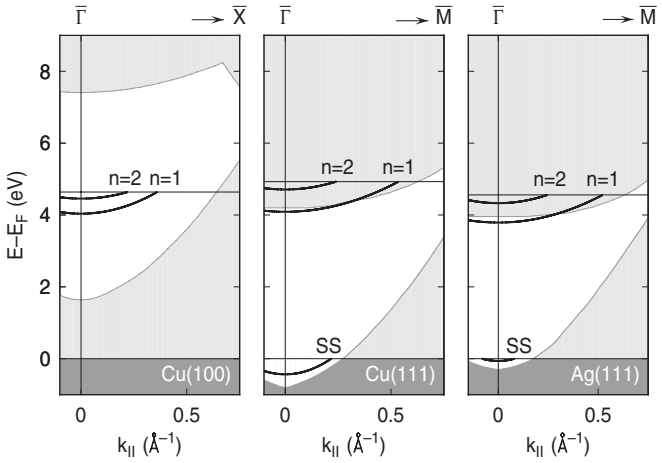

FIG. 1. Projected surface band structure of Cu(100), Cu(111), and Ag(111). Light (dark) grey areas indicate empty (filled) bulk states. Thin lines mark the vacuum level, thick lines close to the vacuum level show the dispersion of the $n = 1$ and $n = 2$ image-potential state/resonance. On Cu(111) and Ag(111), the occupied Shockley surface state (SS, thick line) is supported within the projected bulk band gap close to the Fermi energy.

has a magnitude comparable to the interband decay due to the almost complete spatial overlap of the corresponding charge density distributions. For the clean Cu(100) surface, it was shown that 50% of the increase of the decay rate with the energy of parallel motion $E_\parallel = \hbar^2 k_\parallel^2/2m_0$ is governed by the change of the phase space for interband decay whereas the other half is due to intraband decay.

In contrast to Cu(100) where the vacuum level E_{vac} and therefore the image-potential states are located in the center of the projected bulk band gap (see Fig. 1), the image-potential states can become resonant with the projected bulk conduction band on the (111) noble metal surfaces. As shown for Cu and Ag in Fig. 1, this is the case for $n = 2$ and higher n states over the entire range of the momentum parallel to the surface. The $n = 1$ image-potential state is located inside the projected band gap of the substrate at $\overline{\Gamma}$. With increasing $k_\parallel$, however, it crosses the boundary of the projected band gap and becomes degenerate with unoccupied bulk states. When image-potential states are degenerate with bulk bands, their population can decay via energy-conserving resonant one-electron tunneling through the metal/vacuum interface into the bulk. The image-potential states become quasistationary within the one-electron picture and are then termed image-potential resonances.[5] Despite the additional decay via elastic electron transfer into the bulk, remarkably long lifetimes of image-potential resonances have been observed on Ag(111).[6] It has been suggested[5] that the one-electron and many-body decay rates do not give additive contribution to the decay rate of the image-potential resonances. The decay rate Γ and therefore the linewidth of the image-potential resonances is dominated by the resonance charge transfer rate Γ^{RCT}, which depends on the reflectivity of the metal/vacuum interface.[7] $\tau^{\mathrm{RCT}} = 1/\Gamma^{\mathrm{RCT}}$ defines the time during which an excited electron is trapped in front of the surface. The many-body energy relaxation (decay rate $\Gamma^{e\text{-}e}$) is mainly operative once an electron is transferred into the bulk. Obviously, the appearance of the one-electron decay channel should reveal itself in the $k_\parallel$ dependence of the linewidth of the image-potential resonances on (111) noble metal surfaces. As to the many-body decay, since the bulk penetration of the image-potential states depends on their energetic position within the projected bulk band gap,[8] the inelastic decay rate of the first image-potential state on Ag(111) and Cu(111) is *a priori* sensitive to $k_\parallel$.

A further important difference between the (100) and (111) noble metal surface is the occurrence of the occupied Shockley surface state in the projected band gap below the Fermi energy on the (111) oriented surfaces. This state (SS in Fig. 1) opens an additional surface-located decay channel that might be of great relevance for the inelastic decay of the image-potential states, since the wave functions of the image-potential states and the Shockley state have a strong spatial overlap.[9]

One reason for the fact that there are only few studies on the momentum dependence of decay rates in image-potential states might be connected to experimental challenges: since the lifetimes of electrons in image-potential states are of the order of a few 10 fs, it seems to be difficult to study subtle changes as a function of parallel momentum. An elegant way to reduce and control the coupling of surface states with bulk metal is to introduce thin insulating spacer layers.[10–14] In many cases, this results in a drastic increase of the lifetimes.[15–18] Rare-gas layers are, in particular, attractive for this purpose, since they interact only weakly with the underlying substrate and can be grown with very high order on most flat metal substrates.[19,20] For the typical excitation energies of image-potential states, rare-gas layers do not provide additional decay channels so that the main processes behind the population decay of the image-potential states are the same as for clean surfaces. For thick Ar layers on a Cu(100) surface, it has been already shown that the momentum-dependent decay rate of electronic states located at the rare-gas/metal interface is simply scaled by a common factor compared to the momentum-dependent decay rate of the image-potential states on the clean Cu(100) surface.[21,22]

In this contribution, we present a study of the momentum-dependence of the decay rate of the first $n = 1$ image-potential state on clean and rare-gas covered Ag(111), Cu(111), and Cu(100) surfaces by means of time- and angle-resolved two-photon photoemission spectroscopy. These results are compared with theoretical calculations of the inelastic many-body and resonant one-electron decay rates of excited electrons in image-potential states on Ag(111) and Cu(111) surfaces based on the many-body theory within the self-energy formalism.

II. EXPERIMENT

The experiments have been carried out in a UHV chamber with a base pressure below 5×10^{-11} mbar at room temperature. The samples were prepared by standard sputtering and annealing procedures and could be cooled down to 80 K by using liquid nitrogen or to about 25 K by using liquid helium. Surface cleanliness and order were verified by x-ray photoelectron spectroscopy (XPS), low-energy electron diffraction (LEED), and by linewidth measurements with 2PPE.[23] Atomically flat rare-gas layers were obtained by well defined gas exposures on top of an annealed monolayer, followed by a second annealing step.[24,25] The coverage was

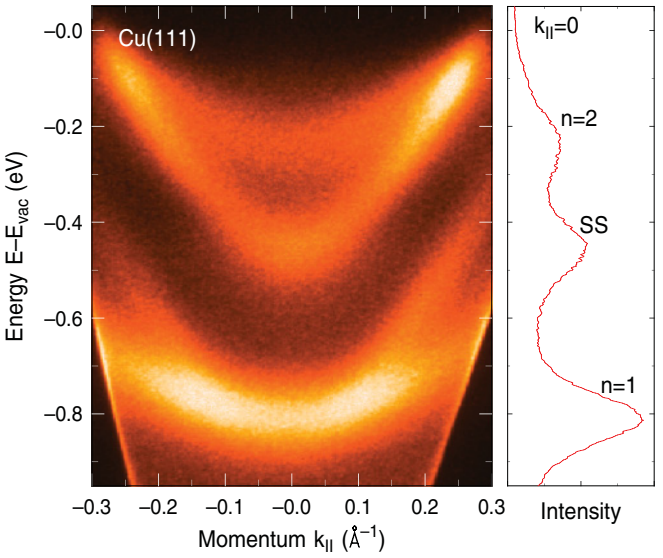

FIG. 2. (Color online) (Left) $E(k_\parallel)$ 2PPE spectrum for the clean Cu(111) surface recorded at 26 K sample temperature. Bright areas indicate high 2PPE intensity. (Right) 2PPE energy spectrum for $k_\parallel = 0$ obtained from a cut through the 2D spectrum with a width of about 0.013 Å^{-1}.

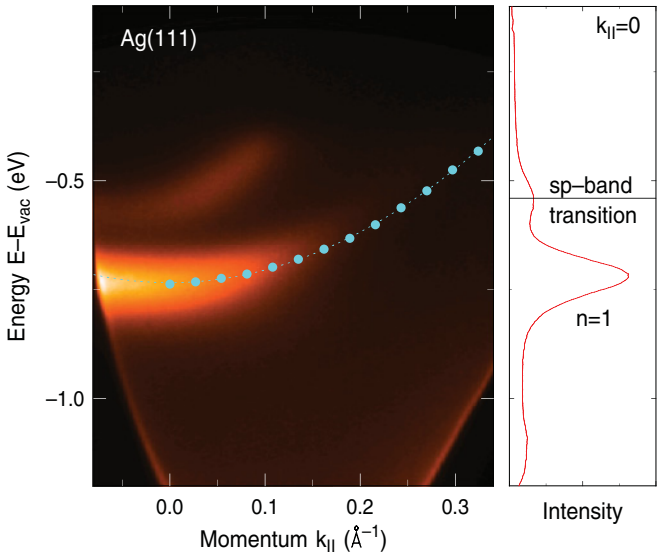

FIG. 3. (Color online) (Left) $E(k_\parallel)$ 2PPE spectrum for the clean Ag(111) surface recorded at 30 K sample temperature. Bright areas indicate high 2PPE intensity. The cyan points mark the position of the $n = 1$ image-potential state/resonance for different parallel momenta obtained from vertical cuts through the spectrum. The dotted line shows a parabolic fit to the data points. (Right) 2PPE energy spectrum for $k_\parallel = 0$ obtained from a cut through the 2D spectrum with a width of about 0.013 Å^{-1}.

calibrated by temperature-programmed desorption (TPD) with an accuracy of 2% of a monolayer.[24]

Two different experimental setups have been used. For parts of the experiments, the optical setup consisted of a commercial 100 kHz Ti:sapphire femtosecond laser system that pumps an optical parametric amplifier generating laser pulses in the visible range with a pulse-length of typical 50 fs (FWHM). Depending on the work function of the samples, the wavelength was tuned between 515 and 580 nm, and the pulse energy was adjusted between 50 and 200 nJ. One part of the visible pulses was frequency doubled in a 100-μm-thick type I BBO crystal generating pulses with frequencies in the ultraviolet range that were used to populate the image-potential states (pump pulses). The other part of the visible pulses were used as probe pulses for photoemission of a fraction of the excited electrons. These pulses could be delayed with respect to the pump pulses by a motor-driven delay stage with a resolution of better than 1 fs.

In this first setup, photoelectrons were detected by a hemispherical analyzer (Specs Phoibos 150) equipped with a two-dimensional (2D) charge-coupled-device (CCD) detector and an angle-resolved lens mode.[21] It allowed for single-shot $E(k_\parallel)$ measurements. At a pass energy of 10 eV, a kinetic energy range of 1.3 eV was visible along the energy-dispersive axis of the spectrometer with an energy resolution of 14 meV. The full acceptance angle of the electron lens was $\pm 13^\circ$ with an angular resolution of better than 0.4°, which corresponds to a momentum resolution of about 0.005 Å^{-1} in the investigated energy range. Figures 2 and 3 display raw 2PPE data for clean Cu(111) and Ag(111). All energies are given with respect to the vacuum level that serves as the reference level for image-potential states. Energy and momentum dispersions were carefully calibrated in a previous work[21] and checked for the experiments carried out here. In order to be independent on the calibration of the momentum scale, we will, however, specify the position within an excited band in the following not by the momentum parallel to the surface $k_\parallel$ but by the energy above the band bottom. For a parabolic band, this energy corresponds to the kinetic energy of parallel motion $E_\parallel = k_\parallel^2/2m_0$.

For the other parts of the experiments, a Ti:sapphire oscillator with a repetition rate of 82 MHz was used. This laser provided pulses with a photon energy around 1.55 eV and a pulse duration of 45 fs. One part of these laser pulses was frequency tripled by subsequent second-harmonic and sum-frequency generation providing photons with a pulse duration of about 60 fs. The other part served as time-delayed probe pulses. For most of the experiments reported here, the photon energy of the frequency-tripled pump pulses was set slightly below the work function of the respective surface in order to excite the complete system of image-potential states up to the vacuum energy and to simultaneously avoid a strong background from one-photon photoemission. In this setup, photoelectrons were detected by a conventional hemispherical electron energy analyzer equipped with channeltron detectors. The energy and momentum resolution were 22 meV and ± 0.015 Å^{-1}, respectively. Time-resolved measurements for different parallel momenta $k_\parallel$ with this experimental setup were performed by rotating the sample.

For the experiments on rare-gas covered Ag(111), a serious restriction for the achievable signal-to-noise ratio was the observation of laser-induced desorption by the visible probe pulses at 100 kHz repetition rate. Laser-induced desorption by the UV pump pulses has already been observed for 2PPE on Ar/Cu(100).[26] In the latter experiment, which has been done with the 82-MHz laser-oscillator system, the Ar desorption has been found to be driven by a single UV-photon excitation as has

been concluded from the observation of a linear dependence of the desorption rate on the UV-laser fluence. This process could be neglected for the experiments on Cu(111) and Ag(111), which have been done with the amplified laser system at a repetition rate of 100 kHz. The higher peak power of the laser pulses in these experiments made it possible to use more than one order of magnitude less average power in for a comparable average 2PPE intensity. For Ar/Ag(111), however, the Ar desorption rate has been found to depend quadratically on the visible probe pulse fluence with its photon energy of 2.14 eV. This process, which has not been observed for Ar/Cu(111) and might be connected to the higher background of secondary electrons, made it necessary to considerably reduce the laser power that went along with a reduced signal-to-noise ratio.

III. THEORY

The calculations of the inelastic decay rate $\Gamma^{e\text{-}e}$ were performed in the self-energy formalism of many-body theory using the GW approximation.[27] The method is described in detail in Refs. 3,28, and here we give just a brief overview. Within this formalism, the inelastic electron-electron scattering contribution to the decay of the electronic state with wave function Ψ_0, energy E_0, and wave vector $\mathbf{k}_0$ is obtained as the projection of the imaginary part of the self-energy operator Σ onto this state (atomic units are used unless otherwise stated):

$$\Gamma^{e\text{-}e}_{\mathbf{k}_0} = -2\langle\Psi_0|\mathrm{Im}\Sigma|\Psi_0\rangle = -2\sum_{n,\mathbf{k}}\int\int[\Psi_0^*(\mathbf{r})\Psi_{n\mathbf{k}}(\mathbf{r}) \times \mathrm{Im}W(\mathbf{r},\mathbf{r}',|E_0 - E_{n\mathbf{k}}|)\Psi^*_{n\mathbf{k}}(\mathbf{r}')\Psi_0(\mathbf{r}')]d^3\mathbf{r}d^3\mathbf{r}'. \quad (1)$$

Here, the self-energy is represented by the first term of the expansion in terms of the screened Coulomb interaction W, which is calculated within the random phase approximation. Summation is carried out over all final electronic states $n\mathbf{k}$ with energies $E_F < E_{n\mathbf{k}} < E_0$. Thus the many-body decay rate is determined by three main factors: (i) the phase space of the final states ($n\mathbf{k}$), (ii) the overlap between the wave functions of the initial and final states, and (iii) the magnitude of the imaginary part of the screened Coulomb interaction ImW. The latter is given in linear response theory by

$$W(\mathbf{r},\mathbf{r}';\omega) = V(\mathbf{r}-\mathbf{r}') + \int\int[V(\mathbf{r}-\mathbf{r}_1) \times \chi(\mathbf{r}_1,\mathbf{r}_2;\omega)V(\mathbf{r}_2-\mathbf{r}')]d^3\mathbf{r}_1d^3\mathbf{r}_2, \quad (2)$$

where $V(\mathbf{r}-\mathbf{r}')$ is the bare Coulomb interaction and $\chi(\mathbf{r}_1,\mathbf{r}_2;\omega)$ is the density-density response function of interacting electron system.

The electronic structure is described by a model pseudopotential $\mathbb{U}(z,k_\parallel)$,[29,30] that varies only in the direction z perpendicular to the surface and remains constant in the plane of the surface. This approximation is justified for both the surface states and the image-potential states. The parameters of the pseudopotential dependent on the wave vector $k_\parallel$ in the direction parallel to the surface were adjusted in such a way that the main features of the experimentally observed band structure are well reproduced for each $k_\parallel$ point of interest: the energies of the edges of the projected bulk band gap, the Shockley surface state, and the first image-potential state. This method has been widely used for calculation of the lifetimes of excitations in surface and image-potential states on close-packed surfaces of various metals.[31]

For Cu(111) and Ag(111) surfaces, we have also calculated the one-electron resonance decay rates Γ^{RCT} of the image-potential resonance issuing from the $n = 1$ parent image-potential state for $k_\parallel$ such that the latter disperses out of the projected band gap. To this end, we have used the wave packet propagation technique, as documented for the image-potential resonances in Ref. 5. In brief, one studies the dynamics of the excited electron in the system described by the one-dimensional Hamiltonian:

$$H = -\frac{1}{2}\frac{\partial^2}{\partial z^2} + \mathbb{U}(z,k_\parallel) + \mathcal{A}(z), \quad (3)$$

where $\mathcal{A}(z)$ is a non-Hermitian absorbing potential allowing to avoid the artificial reflection of the electron wave packet at the grid boundaries as well as to account for the many-body decay of the population inside the metal.[31] The time-dependent Schrödinger equation with Hamiltonian H is solved via a short-time propagation algorithm.[32] The wave function $\Psi(z,t)$ of the excited electron is discretized at a mesh of equidistant points in z coordinate so that the Fourier-grid technique[33] can be used. Provided $\Psi(z,t)$ over large enough time interval, the energies and decay rates of the resonances in the system are extracted from the analysis of the autocorrelation amplitude $\langle\Psi(z,t=0)|\Psi(z,t)\rangle$.[31]

IV. RESULTS AND DISCUSSION

A. Clean Cu and Ag surfaces

Figures 2 and 3 show $E(k_\parallel)$-spectra recorded at zero time-delay between pump and probe pulses for the clean Cu(111) and Ag(111) surface, respectively. For Cu(111), the pump photon energy was set to 4.82 eV, slightly below the work function 4.87 eV of the clean surface.[34] Four different electronic bands can be identified in this spectrum that has been recorded at a sample temperature of 26 K. The two weakly dispersing bands at energies of -0.82 and -0.25 eV at $k_\parallel = 0$ are assigned to the $n = 1$ and $n = 2$ image-potential bands, respectively. Close to the $n = 1$ image-potential band a second structure with a stronger dispersion is visible that can be attributed to a resonant bulk transition.[35] The second, strongly dispersing band originates from the occupied Shockley surface state (SS) located at 0.435 eV below the Fermi energy.[36] Electrons in this state can be emitted by nonresonant 2PPE, thus the 2PPE signal arises at the same final state energy as for photoemission from an intermediate state at -0.45 eV for $k_\parallel = 0$.

For Ag(111), the photon energy of the pump pulses was set to 4.28 eV, significantly below the work function of 4.56 eV[37] of the clean surface and such that the second image-potential state is not being populated. Therefore interband scattering processes between different image-potential states are avoided. The $E(k_\parallel)$ spectrum recorded at 30-K sample temperature (see Fig. 3) shows the dispersion of the first image-potential state $n = 1$ and the resonant bulk transition.[35] In this case, the latter is energetically non degenerate with image-potential states.

The dynamics of the excited states were studied by recording full $E(k_\parallel)$ spectra for different time delays between

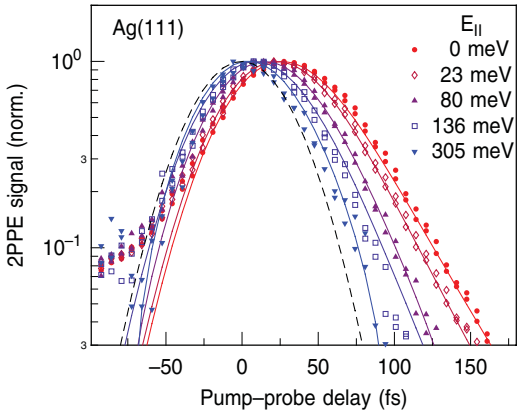

FIG. 4. (Color online) Time-resolved 2PPE traces recorded for the $n = 1$ image-potential state on Ag(111) at 30 K for different momenta parallel to the surface corresponding to different kinetic energies $E_\parallel = k_\parallel^2/2m_0$ of parallel motion (symbols). Thin solid lines show fits using rate equations. The dashed line indicates the cross correlation of pump and probe pulses recorded from the nonresonant 2PPE-signal from the Shockley state.

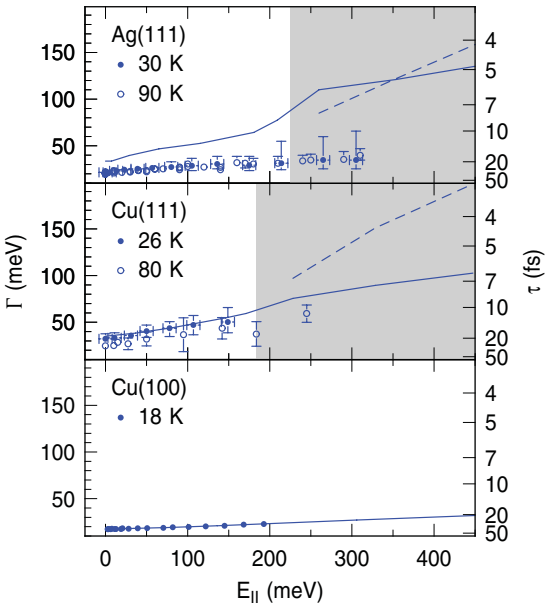

FIG. 5. (Color online) Decay rates $\Gamma = 1/\tau$ of the $n = 1$ image-potential state on Ag(111) and Cu(111) as a function of kinetic energies of parallel motion $E_\parallel = k_\parallel^2/2m_0$ (symbols). Previous results obtained on Cu(100)[4,21] are shown for comparison. For the latter, the error bars are in the order of the symbol size. The solid lines for Ag(111) and Cu(111) are the calculated many-body contributions to the decay, while the dashed lines represent the one-electron decay as described in the text. For Cu(100), the solid line shows the theoretical result from Ref. 4.

pump and probe pulses. Time-resolved pump-probe traces for different parallel momenta, as indicated by the dots in Fig. 3, were determined by integrating the 2PPE intensity of each spectrum within a small rectangular region with an energy width of 30 meV and a momentum width of 0.013 Å^{-1}, respectively.

Exemplary, such time-resolved 2PPE traces are shown in Fig. 4 for the $n = 1$ image-potential state of clean Ag(111). Clearly, the decay after excitation with the UV pump pulse (positive time delays) becomes faster with parallel momentum. The dashed line shows the cross correlation between pump and probe pulses on the sample surface, which represents the time-resolution of the experiment. It has been measured by recording the nonresonant 2PPE signal from the occupied Shockley surface state. From this measurement, the lengths of pump and probe pulse were determined to be typically 50 fs (FWHM). In the case of fast decay, the inelastic lifetime τ (respectively, the decay rate $1/\tau$) has been determined by fitting the data using a rate equation model (solid lines in Fig. 4). In most cases, however, the decay rate could be determined independently from the underlying model to describe the 2PPE process by simply fitting the exponential decay of the signal for time delays that are large compared to the pulse lengths. This has been particularly applied for the rare-gas covered surfaces where long lifetimes have been observed due to the strong decoupling of the image-potential states from the substrate.

For negative time delays, all traces show a slow, exponentially decaying component. Lifetimes derived from this decay depend on the sample temperature, increasing from 160 fs at 300 K to 250 fs at 26 K for the $n = 1$ image-potential state at $k_\parallel = 0$. This component can be attributed to the decay of hot electrons excited by the visible pulse and photoemitted by the UV pulse. This process has been already observed and discussed in previous 2PPE experiments carried out on Ag(100) and Cu(100),[38] significantly stronger visible on Ag(100).

Figure 5 summarizes the experimental and theoretical decay rates for the $n = 1$ image-potential state on the clean Ag(111) and Cu(111) surfaces. The results are plotted as a function of kinetic energy of electron motion parallel to the surface $E_\parallel = k_\parallel^2/2m_0$. Experimental data are shown for two different temperatures. For the sake of comparison, we also reproduce previous results on Cu(100).[4,21] For zero parallel momentum, the lifetimes derived on Cu(111) (≈20 fs at 26 K and ≈25 fs at 80 K) and on Ag(111) (≈31 fs at 30 and 90 K) are in very good agreement with earlier experiments.[39–41] The qualitative dependence of the measured decay rate on $E_\parallel$ is similar on all three surfaces and shows an almost linear increase. Only for small energies of parallel motion the slope is reduced. Compared to Cu(100), the increase of the decay rate with $E_\parallel$ is stronger on the (111) surfaces of Cu and Ag. Within the experimental error the temperature dependence of the decay rates for Cu(111) and Ag(111) seems to be negligible in the range between 26 and 90 K.

The calculated many-body lifetime $\tau = 1/\Gamma^{e\text{-}e} = 19$ fs of the $n = 1$ image-potential state at the $\overline{\Gamma}$ point on Cu(111) is in good agreement with the measured lifetime at the low temperature (20 fs at 26 K). For Ag(111), the calculated many-body lifetimes are somewhat lower than the measured data, i.e., theory overestimates the $\Gamma^{e\text{-}e}$ decay rates. Thus at the $\overline{\Gamma}$ point, the calculated value $\tau = 20$ fs is 1.6 times lower than the experimental value (31 fs at 30 K). This discrepancy is attributed to the neglect of the surface plasmon excitation in the present calculation. In contrast to Cu, the screening of the

d electrons in Ag reduces the energy of the surface plasmon below the energy of the image-potential states. Although this opens a further inelastic decay channel for electrons in the image-potential states, it has been shown that the highly nonlocal character of the self-energy near the surface leads astonishingly to an increase of their lifetime at the $\overline{\Gamma}$ point of silver surfaces.[42,43] *A priori* the surface plasmon excitation channel on silver is also expected to play an important role for $k_{\parallel} \neq 0$.

As can be seen in Fig. 5 on both Cu(111) and Ag(111) surfaces the calculated many-body decay rate $\Gamma^{e\text{-}e}$ grows almost linearly with kinetic energy of parallel motion $E_{\parallel}$. This is in full agreement with experimentally measured trend. For Cu(111), the calculated many-body decay rate perfectly matches the experimental data for $E_{\parallel}$ up to 195 meV. This energy range corresponds to the range of the electron momenta parallel to the surface where the $n = 1$ image-potential state resides in the projected band gap (see Fig. 1). The many-body inelastic electron-electron scattering is then the dominant decay channel for the image-potential state population. For Ag(111), the slope of the calculated $\Gamma(E_{\parallel})$ dependence differs from the measured one. As discussed above, we tentatively attribute the origin of this disagreement to the increasing role of direct interband transitions in the excitation of the surface plasmon with increasing $k_{\parallel}$.

For image-potential states below the gap edge, three channels of many-body inelastic electron-electron scattering are possible. The intraband scattering is operative for the states with $k_{\parallel} \neq 0$. Its contribution to the total decay rate grows with $k_{\parallel}$ due to the increasing number of possible final states. The contribution of this intraband term reaches at maximum $\sim$10% of the total decay rate for the states close to the gap edge for both surfaces.

The interband term is determined by transitions of an excited electron from the image-potential state to bulk states as well as to the Shockley surface state. Because the overlap of the image-potential state and the surface state the contribution of the latter in inelastic decay is quite significant. It amounts $\sim$30–40% of the total inelastic decay rate at the center of the Brillouin zone. When $k_{\parallel}$ increases, the rate of transitions to the surface state slowly increases. On the whole, however, the relative contribution of this process to the total decay rate decreases. Transitions to lower bulk states provide the main contribution ($\sim$60–70% at the $\overline{\Gamma}$ point) to the decay of electrons excited into the $n = 1$ image-potential state. At the $\overline{\Gamma}$ point, the weight of the image-potential state in vacuum equals to 78% and 82% for copper and silver, respectively. However, as the gap edge is approached, this weight drops to $\sim$50%, thus increasing the overlap of the image-potential states with electronic states of the bulk metal. This increasing overlap is mainly responsible for the increase of $\Gamma^{e\text{-}e}$ as a function of $E_{\parallel}$, along with the increase of the phase space of final states for electron transitions.

At large $k_{\parallel}$ the energy dispersion with $k_{\parallel}$ moves the $n = 1$ image-potential state on both, the Cu(111) and the Ag(111), surfaces outside the band gap into the resonance with propagating electronic states of the metal bulk. The decay of the image-potential state population in this case requires a special treatment. Indeed, along with the many-body inelastic decay, the one-electron resonant decay channel into the bulk continuum opens. Image-potential states turn into resonances in one-electron sense for $E_{\parallel}$ above 195 meV for Cu(111) and above 225 meV for Ag(111) surface. When the energy of the image-potential state rises above the band gap edge, the resonant decay rate Γ^{RCT} quickly increases and becomes comparable and then larger than the many body decay rate. In overall, Γ^{RCT} grows 3(3.5) times faster with $E_{\parallel}$ for Ag(Cu) as compared to $\Gamma^{e\text{-}e}$. The wave packet propagation technique calculations performed with and without absorbing potential inside the metal show that in present conditions the one-electron and many-body decay channels do not give additive contribution to the total linewidth as would be observed in spectroscopic experimental design. The total linewidth is given by the resonant decay rate. This finding is in agreement with the previously reported results for image-potential resonances at metal surfaces.[5] Basically, it reflects the fact that the trapping of an electron in front of the surface is due to the finite reflectivity of the metal/vacuum interface. In the framework of the description of the inelastic decay by an optical potential, the many-body process mainly affects the fate of the electron already transferred into the metal, i.e., lost from the point of view of the population of the transient state.

As is shown in Fig. 5 the theoretical calculations predict an accelerated increase of the $\Gamma^{e\text{-}e}$ rate upon crossing the gap edge for Ag(111) and the onset of the rapidly increasing resonant decay rate Γ^{RCT} on both Ag(111) and Cu(111). The measured decay rate, however, shows no effect upon crossing of the gap edge and, rather surprisingly, follows essentially the same dependence on $E_{\parallel}$ as inside the gap. For an explanation, one might consider the possibility that the 2PPE experiment still detects the electron as it is already delocalized into the bulk. Under the present experimental conditions, however, 2PPE is a highly surface specific process because the matrix element between image-potential states and the photoemission final states is appreciable only close to the surface for the 1.5-eV probe photons.[44,45] For that reason, the experiment detects the loss of excited-state surface population due to resonant, elastic electron transfer into the bulk (Γ^{RCT}) in the same way as it detects its loss due to inelastic decay processes $\Gamma^{e\text{-}e}$. In fact, this property of 2PPE has been exploited in several previous experiments that investigated the dynamics of image-potential states and resonances at the Γ point.[6,40,41,46,47] At the moment the difference in calculated and measured gap-threshold behavior of the decay rates is unclear and requires future work.

B. Rare-gas covered surfaces

The influence of rare-gas layers on the momentum dependence of the decay dynamics of the first $n = 1$ image-potential state has been studied for 1 monolayer (ML) Ar, Kr, and Xe on Cu(100), 1–3 ML Ar on Cu(111), and 1ML Ar on Ag(111). As an example, time-resolved 2PPE traces for one monolayer of Krypton adsorbed on Cu(100) are shown in Fig. 6 for different energies of parallel motion. Obviously, even one monolayer of Kr strongly decouples the image-potential state from the metal substrate and leads to much longer inelastic lifetimes as compared to the lifetimes on all three investigated clean surfaces. Again, the decay rate increases significantly with the energy of parallel motion. For time delays larger than about

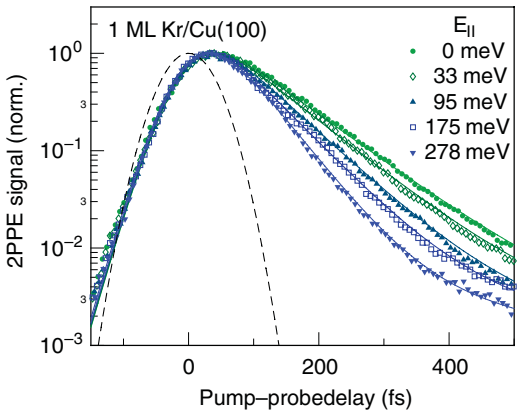

FIG. 6. (Color online) Time-resolved 2PPE traces recorded for the $n = 1$ image-potential state on 1 ML Kr/Cu(100) for different kinetic energies of parallel motion $E_{\parallel} = k_{\parallel}^2/2m_0$ (symbols). Fits using a rate-equation model are drawn as solid lines. The dashed line shows the cross correlation of pump and probe pulses.

350 fs, the time-resolved traces show a weak shoulder, which slows down the decay rate. It is caused by image-potential state electrons primarily excited into the longer-living $n = 2$ state that are resonantly scattered into the $n = 1$ state.[48] This interband scattering process is promoted by steps or surface defects as has been systematically studied by Fauster and Weinelt.[49–51] Since the relative signal arising from this processes is very small, the deduced momentum dependent scattering rates are not affected by this process.

Figure 7 summarizes the results for Cu(100) and shows the momentum-dependent decay rates for one monolayer Krypton and Argon in comparison with the previous results on the clean surface.[4] For both adsorbates, a nearly linear increase of the decay rate with kinetic energies of parallel motion $E_{\parallel}$ is observed. The Ar monolayer leads to the stronger decoupling of the $n = 1$ image-potential state from the metal substrate as compared with the Kr monolayer, and consequently it is

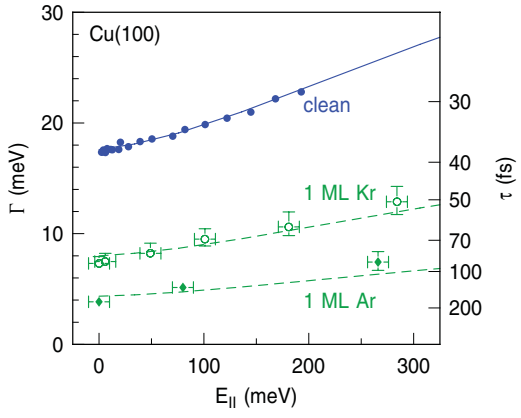

FIG. 7. (Color online) Decay rates $\Gamma = 1/\tau$ of the $n = 1$ image-potential state on Cu(100) covered with 1 ML of Kr and Ar in comparison to previous results obtained on Cu(100)[21] as a function of energy of parallel motion $E_{\parallel}$ (symbols). The solid line shows the theoretical result for clean Cu(100).[4] The dashed lines represent the same curve but scaled by a factor of 2.2 and 4.05, respectively (see text).

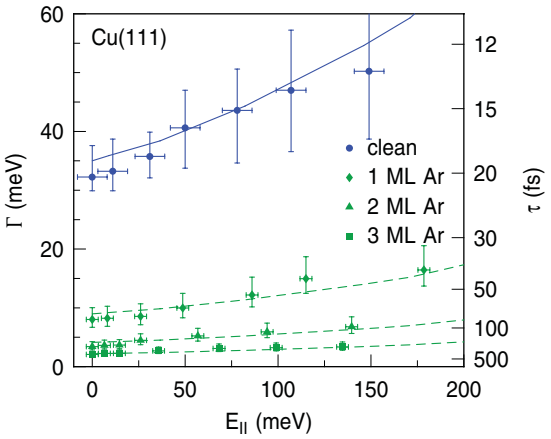

FIG. 8. (Color online) Decay rates $\Gamma = 1/\tau$ of the $n = 1$ image-potential state on clean and Ar-covered Cu(111) as a function energy of parallel motion $E_{\parallel}$ (symbols). The solid line shows the theoretical many-body contributions to the decay rate. The dashed lines for the Ar-covered surface represent the same curve but scaled by a factor of 3.9, 8.5, and 16, respectively.

associated with longer image-potential state lifetimes. This can be qualitatively explained by the different electron affinity of the two rare gases that results in different height of the tunneling barrier for the image-potential state electrons.[18,22] The affinity level of Ar is located 0.25 eV above E_{vac}.[52] Therefore Ar acts as a high tunneling barrier for the whole series of image-potential states. The affinity level of Kr, on the other hand, lies 0.3 eV below E_{vac}[53] and represents a low tunneling barrier only for the $n = 1$ image-potential state. For both rare gases, however, the $n = 1$ image-potential state is still mainly located in the vacuum and shows an effective mass for motion parallel to the surface which is close to the mass of the free electron. A conceivable influence of the incommensurate growth of the rare gas layers on the energy and dynamics of the image-potential states is therefore expected to be negligible.

Remarkably, with the decrease of decay rate from the clean to the Kr- and Ar-covered surface the change of the decay rate with $E_{\parallel}$ is also decreasing. Therefore the decoupling of the image-potential states by the rare-gas layers suppresses the interband scattering in the same way as intraband scattering. This becomes even more obvious from the observation that the $E_{\parallel}$ dependence of $\Gamma^{e\text{-}e}$ for the clean Cu(100) surface as predicted by many-body theory within the GW approximation[4] (solid line) can also successfully describe the experimental data for the Kr- and Ar-covered surface when it is scaled by a constant factor (dashed lines). This scaling law has been found to be also applicable for the momentum-dependent decay rate of electronic states similar to the image-potential states but located at the rare-gas/metal interface, which have been observed for thick Ar layers on Cu(100).[21,22]

The same scaling has been also found for the image-potential states on Cu(111) and Ag(111) as depicted in Figs. 8 and 9. For Cu(111), the electron dynamics in the $n = 1$ image-potential state have been investigated as a function of Ar-layer thickness in the range of 1–3 ML. For all three layer thicknesses, the entire $E_{\parallel}$ dependence of the decay rate scales with almost the same (or only slightly smaller) factor than

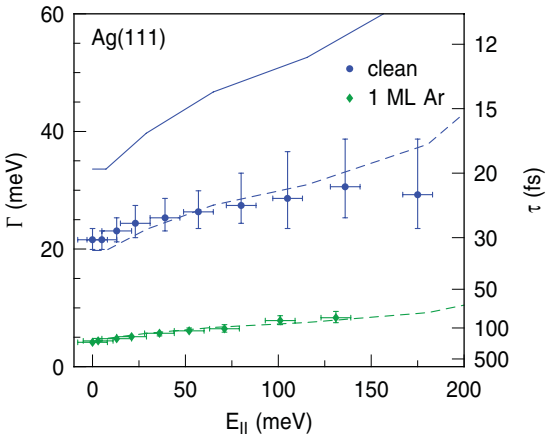

FIG. 9. (Color online) Decay rates $\Gamma = 1/\tau$ of the $n = 1$ image-potential state on clean and Ar-covered Ag(111) as a function of $E_\parallel$. The solid line shows the theoretical many-body contributions to the decay rate. It is scaled to fit the data of the clean surface by a factor of 1.7. For the surface covered with a monolayer of argon, the required scaling factor equals 7.0.

the decay rate at the $\overline{\Gamma}$ point ($E_\parallel = 0$). This is stressed with dashed lines obtained by the scaling of the present theoretical result for the clean Cu(111) surface. Observe, that the scaling holds for a thickness of 3 ML where the $n = 1$ image-potential state becomes energetically degenerate with Cu bulk bands and turns into an image-potential resonance.[46] The change of the character of this state has consequence on the coverage dependence of the inelastic lifetime at the $\overline{\Gamma}$ point.[46] The exponential increase of τ with coverage has different slope in the coverage ranges 1–2 ML and $\geqslant$3 ML, respectively.

The influence of rare-gas layers on the decay rate of the image-potential states can be understood on the basis of the three main factors that determine the many-body decay rate as has been outlined in Sec. III. The decoupling of the image-potential states from the bulk metal by the spacer rare-gas layers primarily reduces the overlap of the image-potential states with bulk states as well as with the Shockley surface state. Within a very crude approximation, this effect reduces to the unique scaling factor appearing in Eq. (1) in front of the corresponding terms in the summation over the final states. Merely, this scaling factor reflects the decrease of the amplitude of the image-potential state wave function Ψ_0 in the metal region. The decrease of the overlap with bulk and surface states significantly reduces the interband contribution to $\Gamma^{e\text{-}e}$. The spacer layers also affect the intraband contribution through $\mathrm{Im}W$. The imaginary part of the screened interaction is determined by the imaginary part of the density-density response function χ [see Eq. (2)], which contains contributions from bulk, surface, and image-potential states. It was shown[43,54] that $\mathrm{Im}W$ decays when moving away from the surface to vacuum. Since rare-gas spacer layers push the image-potential state electron into the vacuum, the intraband scattering rate decreases through the decrease of $\mathrm{Im}W$. Model calculations were also performed to confirm the former discussion. The presence of rare-gas layers was modelled by shifting the image-potential states' wave function away from the bulk metal by a distance of 1–3 interlayer spacing. It was observed that such shift decreases the interband and intraband decay rates by different factors. The decrease factor for intraband decay is ~30% smaller than for interband decay. As far as the intraband scattering determines ~30% of the increase of the linewidth with $E_\parallel$, it is expected that $d\Gamma^{e\text{-}e}/dE_\parallel$ is reduced slightly ($\lesssim$10%) weaker than $\Gamma^{e\text{-}e}(E_\parallel = 0)$ when rare-gas layers are deposited. However, this difference is hard to observe within the accuracy of the present experiment. This might be the reason, why the scaling factors for the measured many-body contributions to the decay rate between the clean and Ar-monolayer covered surfaces, as shown in Figs. 7, 8, and 9, are virtually identical. They are 4.05 for Cu(100), 3.9 for Cu(111), and 4.1 for Ag(111).

V. SUMMARY

In summary, we have shown that the experimentally observed $k_\parallel$ momentum dependence of the decay rate of electrons in the first image-potential state of Cu(111) can be quantitatively described by the many-body theory within the self-energy formalism for those parallel momenta for which the $n = 1$ image-potential state resides in the projected band. In this momentum range, the contribution of the interband decay to the inelastic decay rate is larger as compared to the previously studied Cu(100) surface due to the larger overlap of the image-potential wave function with the Shockley surface state as well as with bulk states. For the clean Ag(111) surface, the agreement between theory and experiment is only qualitative. The theory overestimates the decay rate and its momentum dependence, which can be attributed to the neglect of the surface plasmon excitation channel.

For larger parallel momenta, the $n = 1$ image-potential state on Cu(111) and Ag(111) shifts above the upper edge of the band gap, becomes resonant with projected bulk bands and turns into an image-potential resonance. This opens an additional decay by resonant one-electron decay into the bulk, which has been theoretically treated by performing wave packet propagation calculations. Above the gap edge energy threshold, the theory predicts a rapid increase of the resonant decay rate with a corresponding broadening of the $n = 1$ resonance. We find that the many-body and one-electron decay do not give additive contributions to the linewidth of the state, which appears to be determined by the latter decay channel. The experimentally observed decay rate, however, shows no appreciable effect of gap edge crossing but the same continuous variation as function of $k_\parallel$ over the entire $k_\parallel$ range encompassed in this study.

The decoupling of the $n = 1$ image-potential state by rare-gas layers is found to decrease the inelastic decay rate and its momentum dependence by a common factor for all three investigated surfaces. This has been tentatively ascribed to the decrease of the interband contribution to the total decay rate due to the reduction of the wave function overlap between the image-potential states and the Shockley surface state as well as bulk states.

ACKNOWLEDGMENTS

This work was funded by the Deutsche Forschungsgemeinschaft through GK 790 and GU495/2-1 and by the Ikerbasque Foundation. Support from the University of the

Basque Country (Grant No. IT-366-07), the Departamento de Educacíon del Gobierno Vasco, and the Spanish Ministerio de Ciencia e Innovacíon (Grant No. FIS2010-19609-C02-01) is also gratefully acknowledged.

[1]H. L. Dai and W. Ho, (Eds.), *Laser Spectroscopy and Photo-Chemistry on Metal Surfaces, Part I and II* (World Scientific, Singapore, 1996).
[2]*Dynamics at Solid State Surfaces and Interfaces*, edited by U. Bovensiepen, H. Petek, and M. Wolf (Wiley-VCH, Berlin, 2010), Vol. 1.
[3]P. M. Echenique, R. Berndt, E. V. Chulkov, T. Fauster, A. Goldmann, and U. Höfer, Surf. Sci. Rep. **52**, 219 (2004).
[4]W. Berthold, U. Höfer, P. Feulner, E. V. Chulkov, V. M. Silkin, and P. M. Echenique, Phys. Rev. Lett. **88**, 056805 (2002).
[5]A. G. Borisov, E. V. Chulkov, and P. M. Echenique, Phys. Rev. B **73**, 073402 (2006).
[6]M. Marks, C. H. Schwalb, K. Schubert, J. Güdde, and U. Höfer, Phys. Rev. B **84**, 245402 (2011).
[7]P. M. Echenique and J. B. Pendry, J. Phys. C **11**, 2065 (1978).
[8]P. M. Echenique, J. M. Pitarke, E. V. Chulkov, and V. M. Silkin, J. Electron Spectrosc. Relat. Phenom. **126**, 163 (2002).
[9]J. Osma, I. Sarría, E. V. Chulkov, J. M. Pitarke, and P. M. Echenique, Phys. Rev. B **59**, 10591 (1999).
[10]T. C. Chiang, G. Kaindl, and D. E. Eastman, Solid State Commun. **36**, 25 (1980).
[11]A. P. Alivisatos, D. H. Waldeck, and C. B. Harris, J. Chem. Phys. **82**, 541 (1985).
[12]U. Höfer, M. J. Breitschafter, and E. Umbach, Phys. Rev. Lett. **64**, 3050 (1990).
[13]M. Bertolo, W. Hansen, and K. Jacobi, Phys. Rev. Lett. **67**, 1898 (1991).
[14]C. Keller, M. Stichler, G. Comelli, F. Esch, S. Lizzit, Z. W. Gortel, W. Wurth, and D. Menzel, Phys. Rev. B **60**, 16143 (1999).
[15]A. Hotzel, G. Moos, K. Ishioka, M. Wolf, and G. Ertl, Appl. Phys. B **68**, 615 (1999).
[16]N. H. Ge, C. M. Wong, and C. B. Harris, Acc. Chem. Res. **33**, 111 (2000).
[17]W. Berthold, U. Höfer, P. Feulner, and D. Menzel, Chem. Phys. **251**, 123 (2000).
[18]W. Berthold, F. Rebentrost, P. Feulner, and U. Höfer, Appl. Phys. A **78**, 131 (2004).
[19]J. A. Venables and B. L. Smith, *Rare Gas Solids* (Academic Press, London, 1977), Chap. 10.
[20]H. Schlichting and D. Menzel, Surf. Sci. **272**, 27 (1992).
[21]M. Rohleder, K. Duncker, W. Berthold, J. Güdde, and U. Höfer, New J. Phys. **7**, 103 (2005).
[22]J. Güdde and U. Höfer, Prog. Surf. Sci. **80**, 49 (2005).
[23]C. Reuß, I. L. Shumay, U. Thomann, M. Kutschera, M. Weinelt, T. Fauster, and U. Höfer, Phys. Rev. Lett. **82**, 153 (1999).
[24]W. Berthold, P. Feulner, and U. Höfer, Chem. Phys. Lett. **358**, 502 (2002).
[25]H. Schlichting and D. Menzel, Surf. Sci. **285**, 209 (1993).
[26]W. Berthold, P. Feulner, and U. Höfer, Surf. Sci. **548**, L13 (2004).
[27]L. Hedin, Phys. Rev. **139**, A796 (1965).
[28]P. M. Echenique, J. Osma, M. Machado, V. M. Silkin, E. V. Chulkov, and J. M. Pitarke, Prog. Surf. Sci. **67**, 271 (2001).
[29]E. V. Chulkov, V. M. Silkin, and P. M. Echenique, Surface Science **391**, L1217 (1997).
[30]E. V. Chulkov, V. M. Silkin, and P. M. Echenique, Surface Science **437**, 330 (1999).
[31]E. V. Chulkov, A. G. Borisov, J. P. Gauyacq, D. Sánchez-Portal, V. M. Silkin, V. P. Zhukov, and P. M. Echenique, Chem. Rev. **106**, 4160 (2006).
[32]M. D. Feit, J. A. Fleck Jr., and A. Steiger, J. Comput. Phys. **47**, 412 (1982).
[33]D. Kosloff and R. Kosloff, J. Comput. Phys. **52**, 35 (1983).
[34]Q. Zhong, C. Gahl, and M. Wolf, Surf. Sci. **496**, 21 (2002).
[35]N. Pontius, V. Sametoglu, and H. Petek, Phys. Rev. B **72**, 115105 (2005).
[36]F. Reinert, G. Nicolay, S. Schmidt, D. Ehm, and S. Hüfner, Phys. Rev. B **63**, 115415 (2001).
[37]K. Giesen, F. Hage, F. J. Himpsel, H. J. Riess, and W. Steinmann, Phys. Rev. B **33**, 5241 (1986).
[38]I. L. Shumay, U. Höfer, C. Reuß, U. Thomann, W. Wallauer, and T. Fauster, Phys. Rev. B **58**, 13974 (1998).
[39]E. Knoesel, A. Hotzel, and M. Wolf, J. Electron Spectrosc. Relat. Phenom. **88**, 577 (1998).
[40]M. Weinelt, J. Phys.: Condens. Matter **14**, R1099 (2002).
[41]R. L. Lingle, N. H. Ge, R. E. Jordan, J. D. McNeill, and C. B. Harris, Chem. Phys. **205**, 191 (1996).
[42]A. García-Lekue, J. M. Pitarke, E. V. Chulkov, A. Liebsch, and P. M. Echenique, Phys. Rev. Lett. **89**, 096401 (2002).
[43]A. García-Lekue, J. M. Pitarke, E. V. Chulkov, A. Liebsch, and P. M. Echenique, Phys. Rev. B **68**, 045103 (2003).
[44]U. Höfer, I. L. Shumay, C. Reuß, U. Thomann, W. Wallauer, and T. Fauster, Science **277**, 1480 (1997).
[45]T. Klamroth, P. Saalfrank, and U. Höfer, Phys. Rev. B **64**, 035420 (2001).
[46]A. Damm, K. Schubert, J. Güdde, and U. Höfer, Phys. Rev. B **80**, 205425 (2009).
[47]M. Winter, E. V. Chulkov, and U. Höfer, Phys. Rev. Lett. **107**, 236801 (2011).
[48]W. Berthold, J. Güdde, P. Feulner, and U. Höfer, Appl. Phys. B **73**, 865 (2001).
[49]M. Roth, M. T. Pickel, W. Jinxiong, M. Weinelt, and T. Fauster, Phys. Rev. Lett. **88**, 096802 (2002).
[50]K. Boger, M. Weinelt, and T. Fauster, Phys. Rev. Lett. **92**, 126803 (2004).
[51]T. Fauster, M. Weinelt, and U. Höfer, Prog. Surf. Sci. **82**, 224 (2007).
[52]G. Perluzzo, G. Bader, L. G. Caron, and L. Sanche, Phys. Rev. Lett. **55**, 545 (1985).
[53]N. Schwentner, E. E. Koch, and J. Jortner, *Electronic Excitations in Condensed Rare Gases* (Springer-Verlag, Berlin, 1985).
[54]S. S. Tsirkin, S. V. Eremeev, and E. V. Chulkov, Phys. Rev. B **84**, 115451 (2011).